**SHORT COMMUNICATION**

**DOI: 10.1002/ejic.200800890**

# The Transformation of Core/Shell Aluminium/Alumina Nanoparticles into Nanowires

**Michael Veith,*[a,b] Eve Sow,[a] Ulf Werner,[a] Christian Petersen,[a] and Oral Cenk Aktas[a]**

**Keywords:** $Al/Al_2O_3$ Composite / Nanowires / Catalyst-free nanowire formation / Core-shell structures

Core/shell nanowires of $Al/Al_2O_3$ are obtained by decomposition of *tert*-butoxyalane on metal, silicon or glass substrates heated up to 650 °C without use of a noble metal seed. These biphasic nanowires are characterized by X-ray diffraction (XRD), scanning electron microscopy (SEM), scanning energy dispersive X-ray spectroscopy (EDX), transmission electron microscopy (TEM) and high-resolution TEM. They have uniform diameters of about 20–30 nm, are composed of an inner aluminium wire, wrapped up by aluminium oxide at a constant molar ratio, and have lengths of several micrometers. As the temperatures approach the melting point of Al (660.4 °C), we propose a growth mechanism for the nanowires which resembles to vapour-liquid-solid (VLS) growth of ceramic nanowires with a liquid metal phase catalyst seed which in this case is aluminium. The biphasic nature of the wires is due to the disproportionation of aluminium in the transient "AlO" and to Ostwald ripening.

Aluminium metal is known to have an oxidic protection film on its surface which prevents the metal from further corrosion despite its negative potential towards hydrogen in acidic (–1.676 Volt) and basic (–2.310 Volt) media. This protection coating, so-called "passivation layer", can be further densified in the eloxal process.[1] We have been able to synthesize nanoparticles of aluminium embedded in an alumina matrix, thus protected from further reactions at ordinary conditions (water, oxygen), using a chemical gas-phase reaction as shown in reaction (1).[2–4]

The process shown in Equation (1) uses the volatile single-source precursor *tert*-butoxyalane[3] which, under anaerobic conditions and reduced pressure, reacts to the volatile gases hydrogen and isobutene and to the solid composite $Al/Al_2O_3$, assembling the metal and oxide phases. Contrarily to bulk aluminium (see above), the oxide layer in this nanocomposite (aluminium particle sizes ranging from 1–50 nm, depending on the synthetic conditions)[2–4] is stoichiometric with a molecular ratio of $Al^0/Al^{3+} = 1:2$. A consequence is that the aluminium oxide layer on the spherical particles is quite thick compared to the metallic core (see also below). This contrasts to the findings for bulk aluminium, in which the layer, compared to the metal, is thin.[5]

$$1/2\ [(CH_3)_3C\text{-}O\text{-}AlH_2]_2 \xrightarrow{T > 300\ °C}$$

$$3/2\ H_2 + (CH_3)_2C{=}CH_2 + 1/3\ Al/Al_2O_3 \qquad (1)$$

We wanted to find out if these $Al/Al_2O_3$ core/shell particles, which nicely assemble in a fractal manner on surfaces,[4] could be transformed to other morphologies, especially from zero-dimensional (0-D) to one-dimensional entities (1-D). Since the discovery of carbon nanotubes, one-dimensional structures like nanorods and nanowires are becoming more and more attractive because of their nanoscaled properties.[6,7] In the aluminium/aluminium oxide phase system, either metallic aluminium or oxidic alumina nanowires have been described with respect to their special physical properties like photoluminescence[8–11] and conductivity.[12] Mostly, these one-dimensional entities have been generated by catalyst-supported chemical vapour deposition (CVD)[8,13,14] using particles different from the source material as catalytic seeds or by in situ displacement and template assisted approaches.[7,15,16] So far, there is no report on direct deposition of $Al/Al_2O_3$ core/shell nanowires, although catalyst-free growths of nanowires like ZnO are principally known.[17] In this preliminary state, we were not interested to grow equidistant wires, as our principal objective to these wire-composed surfaces was, apart from others, their use as an overall adherence layer for cells.[18]

Our access to $Al/Al_2O_3$ core/shell nanowires is very simple using the same synthetic process as described in Equation (1) but different conditions. The process is summarized in Equation (2).

$$\text{0-D}\ Al/Al_2O_3 \xrightarrow[T > 490\ °C]{[(CH_3)_3C\text{-}O\text{-}AlH_2]_2} \text{1-D}\ Al/Al_2O_3 \qquad (2)$$

---

[a] INM – Leibniz Institute for New Materials, Campus D2 2,
66123 Saarbrücken/Germany
Fax: +49-681-9300-223
E-mail: michael.veith@inm-gmbh.de
[b] Institute for Inorganic Chemistry, Saarland University,
Postfach 15 11 50, 66041 Saarbrücken/Germany

Apparently, no external catalyst is needed in this process – unlike with comparable growth of one-dimensional metal oxides using noble metals like gold as nucleation seed [Vapour Liquid Solid (VLS) mechanism].[19] In Figure 1, material obtained at 300 °C [Equation (1)] and such obtained at 550–600 °C [Equation (2)] is shown using SEM. While spherical particles appear at 300 °C, only spaghetti-like nanowires are found at the higher temperature.

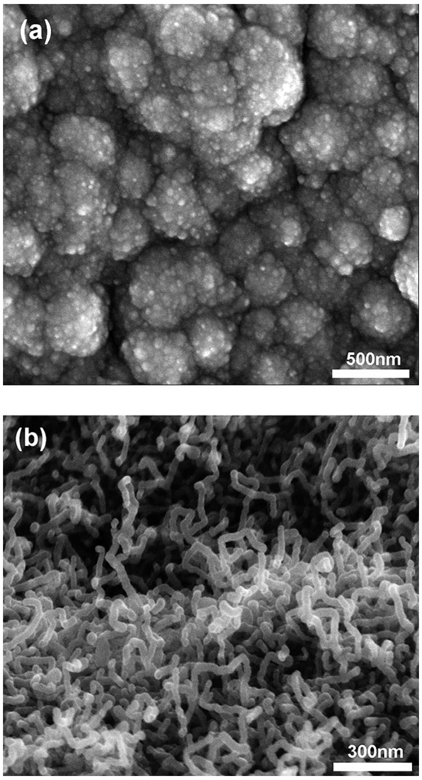

Figure 1. SEM-images of (a) $Al/Al_2O_3$ nanoballs (obtained at 300 °C) and (b) $Al/Al_2O_3$ nanowires (obtained at 550–600 °C) on a steel target. The magnification factor is comparable.

The as-prepared one-dimensional core/shell wires have been analysed using different techniques such as XRD, TEM, XPS and EDX. In Figure 2, XRD of the as-deposited film on steel is shown with reflections due to crystalline aluminium (besides those of the substrate) and an amorphous background.

The growth of the aluminium core structures can be related to the temperature as found from the insert of Figure 2. Whereas in films deposited at low temperature (450 °C) almost no crystalline aluminium can be detected (consistent with particles giving no diffraction due to their small dimensions and/or low crystallinity), diffraction peaks clearly show up at films deposited at temperatures above 550 °C.

The amorphous background is $Al_2O_3$ as found from XPS without carbon contamination (not shown here).[20] In the TEM image of the wires using EDX, one can determine that the shell of the wire is composed of $Al_2O_3$, while the core consists of aluminium (Figure 3 and Figure 4, a, b). HR-TEM images show at some instances the lattice planes of aluminium together with crystalline $Al_2O_3$ which from the lattice distances can either be attributed to the γ- or δ-phase (Figure 5).

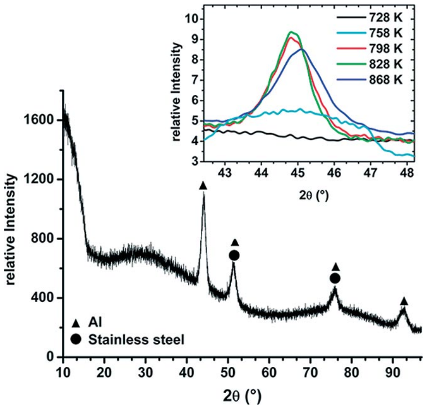

Figure 2. XRD (Co-$K_\alpha$ radiation) of $Al/Al_2O_3$ film deposited on a steel substrate. Insert: The [111] diffraction peak of aluminium from $Al/Al_2O_3$ films obtained at different temperatures.

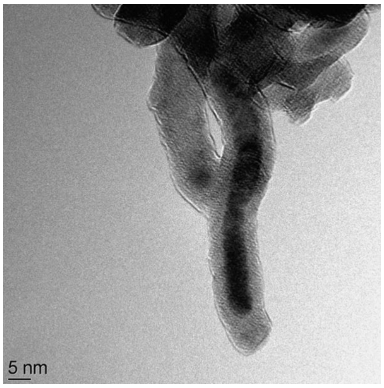

Figure 3. TEM image of an $Al/Al_2O_3$ nanowire using phase contrast (dark inner core is aluminium while the lighter shell is alumina).

Using several images of nanowires like that of Figure 3, we have found out that there is a constant ratio between the radius of the core $r(Al)$ and the total radius of the core/shell $R(Al/Al_2O_3)$ wire, $r(Al)/R(Al/Al_2O_3)$. With the help of interference contrasts in the two-dimensional cut, we determined that this ratio, $r(Al)/R(Al/Al_2O_3)$, is ca. 0.47 which matches nicely with the calculated value of 0.53 using a coaxial composite cylinder model for the Al ($\rho = 2.70\ g\,cm^{-3}$) core surrounded by $\gamma$-$Al_2O_3$ ($\rho = 3.97\ g\,cm^{-3}$) shell in a 1:1 molar ratio. The corresponding ball-like core-shell entities also exhibit a similar ratio $r(Al)/R(Al/Al_2O_3)$ between the inner Al ball and the $Al_2O_3$ shell but at a different experimental value of 0.65 which corresponds perfectly to the calculated value 0.65, assuming a stoichiometric molar ratio of $Al/Al_2O_3$ = 1:1 in the 0-dimensional spheres like in the cylinder model.

At a closer look, in the SEM and TEM images at higher magnification the structures of the wires can be described as cylinders and many of them have ball-like tips. In Figure 6, one of these tips is shown in HR-TEM. It has a crys-

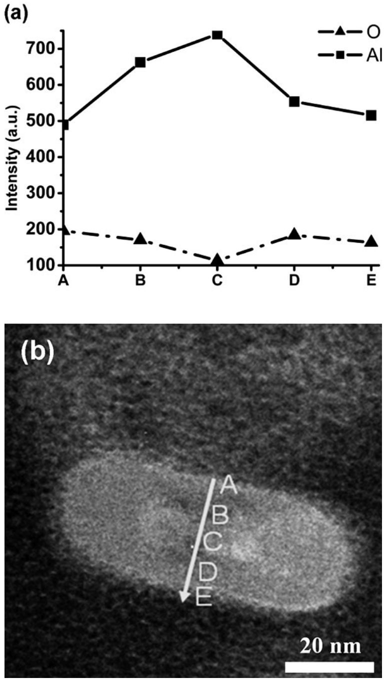

Figure 4. (a) EDX analysis of a wire section [see TEM picture (b)]; oxygen and aluminium contents are given as plots in arbitrary units. (b) Wire cut perpendicular to its length. The letters A, B, C, D, E refer to the places where the analysis has been performed.

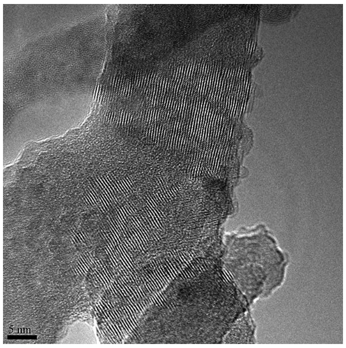

Figure 5. Crystalline $Al_2O_3$ regions on nanowires as found from HR-TEM analysis. The lattice spacings correspond either to γ- or δ-$Al_2O_3$.

talline aluminium core, as deduced from the lattice spacings and from electron diffraction. This core is surrounded by further crystallites (see curvature in the figure) which from their lattice spacings and diffraction belong most likely to δ-$Al_2O_3$ (some γ-$Al_2O_3$ might also be included). The cylinder attached to the tip is made of the core-shell nanowire as discussed before.

From these findings, we propose a growth mechanism which is valid for temperatures around 610 ± 50 °C. This mechanism resembles the VLS growth of ceramic nanowires with a liquid metal phase as catalyst and seed.[19] In contrast to this mechanism, the metallic aluminium itself serves as a catalyst that is formed from the phase-separated metal entities in the fractal ball-like entities[2] by an arrangement which reminds of Ostwald ripening[21] (the melting point of pure bulk aluminium is 660.4 °C). Depending on the primary ball-like core-shell $Al/Al_2O_3$ particle size, the typical wires grown with this process have diameters from 10–40 nm and lengths up to several µm (the aspect ratio is therefore more than one thousand). At a constant pressure and temperature, a reproducible diameter of the wires can be obtained, an expansion of both parameters leading to thicker or longer wires. Eventually, one ball seed may produce several wires, as found in Figure 7, and the flow rate of the precursor $(t\mathrm{BuOAlH}_2)_2$ affects the density of the structures.

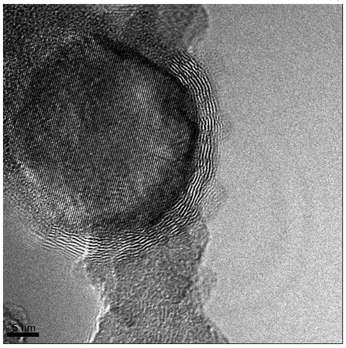

Figure 6. The tip of a nanowire in HR-TEM. The spherical core entity is aluminium due to the spacings of the lattice and due to EDX. In the enveloping outer shell, many differently orientated crystallites may be recognized with lattice spacing typical for γ- or δ-$Al_2O_3$.

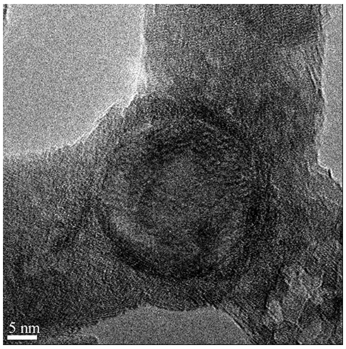

Figure 7. HR-TEM picture of a junction of three nanowires. The junction part is made of a ball, the core of which is pure aluminium.

To conclude, it seems clear that intermediate metastable “AlO” could be the driving force of $Al/Al_2O_3$ balls or wires. This formal $Al^{2+}$ should stabilize by disproportionation into $Al^0$ and $Al^{3+}$, giving a stoichiometric ratio of $Al^0$ and $Al^{3+}$ of 1:2. This resembles findings from silicon/siliconoxide core/shell particles and wires which are thought to evaluate from intermediate SiO by disproportionation into $Si^0$ and $Si^{4+}$.[22]

## Acknowledgments

The authors would like to thank the Deutsche Forschungsgemeinschaft (DFG) (SFB 277, SP 1181 and GRK 532) for financial support, as well as Prof. Dr. F. Mücklich, Saarland University, Saarbrücken, for providing facilities.

[1] R. J. P. Williams, *Coord. Chem. Rev.* **2002**, *228*, 93–96.

[2] M. Veith, *Top. Organomet. Chem.* **2005**, *9*, 81–100.

[3] M. Veith, *J. Chem. Soc., Dalton Trans.* **2002**, *12*, 2405–2412.

[4] M. Veith, K. Andres, S. Faber, J. Blin, M. Zimmer, Y. Wolf, H. Schnöckel, R. Köppe, R. d. Masi, S. Hüfner, *Eur. J. Inorg. Chem.* **2003**, *24*, 4387–4393.

[5] A. Nylund, I. Olefjord, *Surf. Interface Anal.* **1994**, *21*, 283–289.

[6] Y. Xia, P. Yang, Y. Sun, Y. Wu, B. Mayers, B. Gates, Y. Yin, F. Kim, H. Yan, *Adv. Mater.* **2003**, *15*, 353–389.

[7] J. Hu, T. W. Odom, C. M. Lieber, *Acc. Chem. Res.* **1999**, *32*, 435–445.

[8] X. S. Fang, C. H. Ye, X. X. Xu, T. Xie, Y. C. Wu, L. D. Zhang, *J. Phys. Condens. Matter* **2004**, *16*, 4157–4163.

[9] Q. Zhao, *Met. Soc. China* **2005**, *15*, 306–309.

[10] D. H. L. Ng, P. Yu, N. G. Ma, C. K. Lo, W. Y. Kwok, M. Y. Yau, C. Y. To, T. K. Li, C. J. Deng, *J. Eur. Ceram. Soc.* **2006**, *26*, 1561–1565.

[11] C. Y. To, L. Y. Cheung, Y. F. Li, K. C. Chung, D. H. C. Ong, D. H. L. Ng, *J. Eur. Ceram. Soc.* **2007**, *27*, 2629–2634.

[12] Y. Wang, Z. L. Ma, C. Berta, *Solid State Commun.* **2004**, *129*, 681–685.

[13] X. S. Fang, C. H. Ye, X. S. Peng, Y. H. Wang, Y. C. Wu, L. D. Zhang, *J. Mater. Chem.* **2003**, *13*, 3040–3043.

[14] S. Han, C. Li, Z. Liu, B. Lei, D. Zhang, W. Jin, X. Liu, T. Tang, C. Zhou, *Nano Lett.* **2004**, *4*, 1241–1246.

[15] A. Hoffman, A. Heiman, H. P. Strunk, S. H. Christiansen, *J. Appl. Phys.* **2002**, *91*, 3336–3344.

[16] M. H. Huang, S. Mao, H. Feick, H. Yan, Y. Wu, H. Kind, E. Weber, R. Russo, P. Yang, *Science* **2001**, *292*, 1897–1899.

[17] M. Veith, C. Petersen, O. C. Aktas, W. Metzger, M. Oberringer, T. Pohlemann, M. Müller, S. Gerbes, *Mater. Lett.* **2008**, *62*, 3842–3845.

[18] X. Zhang, L. Wang, G. Zhou, *Rev. Adv. Mater. Sci.* **2005**, *10*, 69–72.

[19] Y. Wu, P. Yang, *J. Am. Chem. Soc.* **2001**, *123*, 3165–3166.

[20] E. Sow, Ph. D. Thesis, Saarland University, Saarbrücken, Germany, **2008**.

[21] G. D. Lilly, J. Lee, K. Sun, Z. Tang, K. S. Kim, N. A. Kotov, *J. Phys. Chem. C* **2008**, *112*, 370–377.

[22] N. Wang, Y. H. Tang, Y. F. Zhang, C. S. Lee, I. Bello, S. T. Lee, *Chem. Phys. Lett.* **1999**, *299*, 237–242.

Received: September 4, 2008